Published in final edited form as:
Cancer Res. 2008 March 1; 68(5): 1267–1274. doi:10.1158/0008-5472.CAN-07-2304.

Rad9 Has a Functional Role in Human Prostate Carcinogenesis

Aiping Zhu[1], **Charles Xia Zhang**[1], and **Howard B. Lieberman**[1,2]

[1]Center for Radiological Research, Columbia University, College of Physicians and Surgeons, New York, New York

[2]Department of Environmental Health Sciences, Columbia University, Mailman School of Public Health, New York, New York

Abstract

Prostate cancer is currently the most common type of neoplasm found in American men, other than skin cancer, and is the second leading cause of cancer death in males. Because cell cycle checkpoint proteins stabilize the genome, the relationship of one such protein, Rad9, to prostate cancer was investigated. We found that four prostate cancer cell lines (CWR22, DU145, LNCaP, and PC-3), relative to PrEC normal prostate cells, have aberrantly high levels of Rad9 protein. The 3′-end region of intron 2 of *Rad9* in DU145 cells is hypermethylated at CpG islands, and treatment with 5′-aza-2′-deoxycytidine restores near-normal levels of methylation and reduces Rad9 protein abundance. Southern blot analyses indicate that PC-3 cells contain an amplified *Rad9* copy number. Therefore, we provide evidence that Rad9 levels are high in prostate cancer cells due at least in part to aberrant methylation or gene amplification. The effectiveness of small interfering RNA to lower Rad9 protein levels in CWR22, DU145, and PC-3 cells correlated with reduction of tumorigenicity in nude mice, indicating that Rad9 actively contributes to the disease. Rad9 protein levels were high in 153 of 339 human prostate tumor biopsy samples examined and detectable in only 2 of 52 noncancerous prostate tissues. There was a strong correlation between Rad9 protein abundance and cancer stage. Rad9 protein level can thus provide a biomarker for advanced prostate cancer and is causally related to the disease, suggesting the potential for developing novel diagnostic, prognostic, and therapeutic tools based on detection or manipulation of Rad9 protein abundance.

Introduction

Prostate cancer is the most prevalent type of neoplasm, other than skin cancer, found in American men and is now the second leading cause of death in this group of individuals. Therefore, the development of better diagnostic or therapeutic strategies is of great concern.

The molecular underpinnings of prostate disease are not completely defined. Several genes have been implicated in the disease process, including *PTEN* (1), *c-myc* (2), and *insulin-like growth factor-I* (3). Regulation of androgen receptor (AR) by genes, such as *Wnt1*, is also likely to affect prostate cancer pathogenesis (4). Mouse models have contributed to understanding the effect of genotype on prostate cancer development (for review, see refs. 5, 6). A few studies have found associations between certain chromosome aberrations and prostate cancer. Loss of chromosome 8p23.2 is associated with advanced stage disease, and

Requests for reprints: Howard B. Lieberman, Center for Radiological Research, Columbia University College of Physicians and Surgeons, 630 W. 168th Street, New York, NY 10032. Phone: 212-305-9241; Fax: 212-305-3229; lieberman@cancercenter.columbia.edu..

gain in 11q13.1 is linked to stage-independent and grade-independent postoperative recurrence (7).

HRAD9 is an evolutionarily conserved human gene first identified as a genetic element important for promoting resistance to DNA damage and regulating cell cycle checkpoints (8). Subsequent analyses indicated that it had a much broader range of activities (for review, see ref. 9). The encoded protein can induce apoptosis (10) and regulate genomic stability (11). It has 3′ to 5′ exonuclease activity (12), can bind p53 consensus DNA-binding sequences and up-regulate transcription of *p21*, as well as other downstream genes (13–15), is able to stimulate the carbamoyl phosphate synthetase activity of CAD protein (16), required for *de novo* synthesis of pyrimidine nucleotides and cell growth, and can bind and stimulate activity of several DNA repair proteins involved primarily in base excision repair (17–23). It also helps stabilize telomeres and participates in recombinational repair of damaged DNA (24). Moreover, at least related mouse Mrad9 is critical for embryogenesis (11). Human Rad9 protein has also been linked to AR. AR is critical for differentiation, growth, and maintenance of the prostate. AR can bind androgen (i.e., testosterone or the more active form DHT), whereas the receptor undergoes a conformational change, moves from cytoplasm to nucleus, and transcriptionally activates genes containing androgen-responsive consensus sequences. AR can bind human Rad9 (25, 26). Moreover, the binding represses androgen-induced AR transcription activity in prostate cancer cells, thus altering prostate function.

We investigated the relationship between prostate cancer and human *Rad9* expression, based primarily on functions of Rad9 protein in maintaining genomic integrity and on its ability to regulate AR transactivity. We report herein that prostate cancer cells express *Rad9* at aberrantly high levels, and such overexpression can be due at least in part to abnormal methylation or gene amplification. We also found that the degree to which small interfering RNA (siRNA) reduces Rad9 protein levels correlates with the extent of decrease in tumorigenicity of these cells after injection into nude mice. We found that the ability of Rad9 to bind to AR and alter its transactivity is not universally relevant to prostate cancer since there was no correlation in the prostate cancer cell lines tested with respect to levels of Rad9, levels of AR, expression of PSA, a downstream target of AR transactivity, and the ability of the cells to form tumors in nude mice. We detected high Rad9 protein levels in 153 of 339 human prostate adenocarcinomas, but just low abundance in 2 of 52 normal prostate tissue controls. Relatively higher levels of Rad9 protein were in general associated with more advanced disease. Our results indicate that Rad9 plays a functional role in prostate carcinogenesis and thus could serve as a biomarker for advanced prostate cancer, as well as potentially a target for therapeutic intervention.

Materials and Methods

Cells, culture conditions, and 5′-aza-2′-deoxycytidine treatment

Prostate cancer cell lines, CWR22, DU145, LNCaP, and PC-3, were grown at 37°C, 5% CO_2 in RPMI 1640 (Invitrogen Corp.), supplemented with 10% fetal bovine serum (FBS). Normal prostate epithelial cells (PrEC; Cambrex, Inc.) were grown in PrEGM Bulletkit medium, serum-free (Cambrex, Inc.) at 37°C, 5% CO_2.

Cells were treated with the demethylating agent 5′-aza-2′-deoxycytidine (Sigma-Aldrich Corp.; 0.25 mmol/L, 200 mmol/L stock in DMSO) as published (27). Control cells were treated with an equivalent amount of DMSO alone. Media were changed daily during the 4-day treatment period. Then, cells were collected using trypsin-EDTA for DNA and protein isolation.

Prostate tissue samples

Human prostate tissue arrays were obtained from Imgenex Corp. and US Biomax, Inc. Sample slides contained 391 human prostate tissue thin sections. The majority of sections (335) were prostate adenocarcinomas representing stages I through IV from different patients, and there were four independent metastases. There were 52 normal prostate tissues, derived from a subset of the population with prostate adenocarcinomas, as well as from unrelated individuals. Dr. Harshwardhan M. Thaker, a pathologist at Columbia University, checked to confirm that the specimens contained cancerous or normal prostate tissues as indicated by the commercial vendors. No patient identifiers were available.

Southern blotting, Western blotting, quantitative reverse transcription–PCR and immunohistochemistry

For Southern blotting, genomic DNA was isolated from prostate cells. DNA (5 μg) was digested with *Eco*RI, fractionated on a 0.7% agarose gel, transferred to a nylon membrane, and hybridized to a ^{32}P-labeled full-length *HRAD9* cDNA or β-actin (internal control) 540 bp PCR product (primers for amplification were 5′-GTTGCTATCCAGGCTGTGC-3′ and 5′-GCATCCTGTCGGCAATGC-3′; see ref. 28) probe at 65°C overnight. The membrane was then washed using a standard protocol (Amersham Biosciences). X-ray film was exposed to the membrane for 1 to 2 days. After developing the film, band intensities were analyzed with Image J (NIH).

For Western blotting, 2×10^5 pelleted prostate cells were lysed in 1 × SDS sample buffer with 5% 2-mercaptoethanol. Twenty-microliter volumes were taken for each sample, boiled 5 min, and subjected to SDS-PAGE (4–20%; Invitrogen Corp.). After electrophoresis, samples were transferred to a polyvinylidene difluoride membrane by electroblotting for 30 min. Blots were blocked by 5% nonfat milk and probed with monoclonal mouse anti-human Rad9 antibody (BD Biosciences) and goat anti-human actin antibody (Santa Cruz Biotechnology, Inc.), followed by addition of secondary antibody conjugated with HPR. Enhanced chemiluminescence Western blotting substrate (Pierce, Inc.) was used to detect protein bands.

For quantitative real-time PCR, RNA was isolated from prostate cells using TRIzol (Invitrogen Corp.), as per the manufacturer's instructions. RNA (5 μg) was reverse-transcribed into cDNA using the superscript II First Strand Synthesis System (Invitrogen Corp.). cDNA was used to amplify *HRAD9* by PCR. DNA primers for the reaction were 5′-TCTGCCTATGCCTGCTTTCTCT-3′ and 5′-AGCGGAAGACAGACAGGAAAGAC-3′. Glyceraldehyde-3-phosphate dehydrogenase (GAPDH) served as an internal reference gene to normalize measurement of *HRAD9* RNA abundance. DNA primers for *GAPDH* were purchased from Super Array, Inc. (UNiGene no. Hs.544577, RefSeq Accession no. NM_002046.2). Quantitative real-time PCR was performed in 25 μL using the SYBR Green PCR Master Mix kit (Applied Biosystems). PCR trials were carried out in triplicate in the Applied Biosystems 7300 real-time PCR system (ABI). PCR conditions were 1 cycle of 50°C for 2 min, 1 cycle of 95°C for 10 min, and 55 cycles of 95°C for 15 s, 60°C for 30 s, and 72°C for 45 s. Relative quantification of *HRAD9* RNA abundance was analyzed by the comparative threshold cycle (C_t) method (29).

Prostate cells were split into two-well chamber slides in preparation for immunohistochemical staining. When cells reached 50% confluence, they were fixed with 4% PFA and 0.02% NP40 overnight, then washed in PBS (1×) with 0.01% Tween 20. Vectastain elite avidin-biotin complex method (ABC) kit was used for immunostaining (Vector Laboratories, Inc.). Cells were washed twice for 5 min after fixation. For quenching of endogenous peroxides, slides were immersed in 3% hydrogen peroxide solution for 5 min

and washed again twice for 5 min and then blocked with normal serum (1:50 from ABC kit; Vector Laboratories, Inc.) at room temperature for 30 min. Slides were incubated with monoclonal antihuman Rad9 primary antibody (1 to 100 dilution; BD Biosciences) overnight at 4°C and washed 3 × 5 min, incubated with biotin-conjugated secondary antibody for 30 min at room temperature, washed again for 3 × 5 min, and then further incubated with ABC for 30 min at room temperature. After washing 3 × 5 min, slides were incubated in fresh diaminobenzidine tetrahydrochloride substrate solution for 5 min. The reaction was stopped by washing in tap water. Counterstaining was performed with Meyer's hematoxylin. Dehydration was carried out in 75%, 80%, 95%, and 100% ethanol, sequentially, followed by soaking in xylene, and mounting coverslips with Permount.

For immunostaining of prostate tissue array slides, deparaffinization, hydration, and immunohistochemistry protocols supplied by Imgenex were followed, and then slides were deparaffinized in Safeclear II reagent (Fisher Scientific Co.) and rehydrated with 100% ethanol, then 95%, 75%, and finally 50% ethanol. Citrate buffer (0.01 mol/L, pH 6.0) was used for antigen retrieval. Immunohistochemical staining procedures, as described above, were then followed.

Methylation at CpG islands

Genomic DNA from prostate cells was extracted using the DNeasy tissue kit (Qiagen, Inc.). Primary normal and cancerous biopsy samples were scraped from slides after deparaffinization and processed for DNA purification, as per cell samples. Methylation status of *HRAD9* CpG islands was determined using the sodium bisulfite sequencing method. Genomic DNA (2 μg) was subjected to bisulfate modification using the EZ DNA methylation kit (Zymo Research Corp.), following the manufacturer's instructions. Bisulfate-treated DNA (4 μL) was amplified in 25 μL containing 1× reaction buffer, 3 mmol/L $MgCl_2$, 0.2 mmol/L each deoxynucleotide triphosphate, 1.5 units expand high-fidelity Taq DNA polymerase (Roche), and 0.3 μmol/L each forward and reverse primer. *HRAD9* CpG islands span over 900 bp from the promoter region to intron 2 of the gene (27, 30). This region was amplified as two overlapping DNA fragments. The first region contained the proximal *HRAD9* promoter and part of exon 1 from –421 to 13 (“A” in the start codon ATG is +1). The second region spanned from –8 to 559 and included part of the proximal promoter through most of intron 2. These two regions were amplified by nested PCR. First round PCR condition was hot start at 95°C for 5 min, then 40 cycles at 94°C for 30 s, 52°C for 45 s, and 72°C for 1 min, and a 10-min final extension at 72°C. One microliter was then diluted 400-fold and used as template in the nested PCR reaction. The PCR condition was hot start at 95°C for 5 min, 35 cycles at 94°C for 30 s, 56°C for 30 s, 72°C for 1 min, and a 7-min final extension at 72°C. Nested PCR products were purified with the GFX PCR DNA and gel band purification kit (Amersham Biosciences) and then cloned into pGEM-T Easy (Promega). T-A plasmid constructs were transformed into *Escherichia coli* JM109 competent cells (Promega). Ten independent bacterial colonies, derived from each construct, were picked and purified, and DNA was isolated from them using the Miniprep kit (Qiagen). DNA samples were sent to the Columbia University DNA Sequence Facility for sequence determination using a SP6 primer (pGEM-T Easy vector has T7 and SP6 promoters). Cytosine methylation of each CpG island dinucleotide was determined by checking the cytosine signal at CpG island positions. Primer pairs for PCR and nested PCR were 5′-TAAGTGGGTGATTTTAGAGAGTT-3′ (Rad9-PF; –420 to –398) and 5′-CCTCCAAAAATTCCAAATAAAACT-3′ (Rad9-PR; +159 to +182), 5′-TAAGTGGGTGATTTTAGAGAGTT-3′ (Rad9-PF; –420 to –398) and 5′-CCAAACACTTCATACTACCCCAA-3′ (Rad9-PRn; –10 to +13), 5′-GGAGAGTTGGGTAGTGTTGG-3′ (Rad9-IF; –43 to –24) and 5′-CCTTCATCAAAATCTTACAAC-3′ (Rad9-IR; +619 to +639), 5′-

GGGGTAGTATGAAGTGTTTGGTTA-3′ (Rad9-IFn; –8 to +16) and 5′-CCCAACCCTCTAACTACTTCTACTC-3′ (Rad9-IRn; +535 to +559).

Tumorigenicity of human prostate cells in nude mice

Human prostate cells (6×10^6 per test site) were suspended in sterile PBS (0.2 mL) and injected into the back of nude mice subcutis. Nude mice were Harlan Sprague-Dawley, Inc., Nu/Nu males, of ages 4 weeks old. Each mouse was injected at two to four different sites to reduce the number of animals needed. In pilot studies with normal (PrEC) and tumor (CWR22, DU145, PC-3) cells, there was no detectable difference in tumor formation whether one or up to four sites per animal were injected. Tumors were detectable, initially assessed, and measured usually after 2 to 3 weeks postinjection. Tumor size was measured every 5 days with a vernier caliper by two investigators blinded, such that mouse identities were coded and unknown until the experiment ended. Tumor volume was calculated based on the average of the two sets of measurements. Tumors were dissected from animals and saved in 10% formaldehyde. Tumor thin sections were stained with H&E to view histologic morphology and with antibodies against human epithelial cell–specific markers (i.e., cytokeratin 5, 18, 19; Sigma) using the ABC kit (Vector Laboratories) and procedures used to stain tissue microarrays to confirm their human origin.

HRAD9 siRNA viral vector, recombinant virus, and infection of prostate cancer cells

The *HRAD9* siRNA target sequence (AGGCCCGCCAUCUUCACCA) was designed and synthesized by Oligoengine, Inc. pSUPER.retro.puro siRNA expression vector (Oligoengine, Inc.) was used to construct a *HRAD9* siRNA plasmid, which was transfected into the retrovirus packaging phi-NX cell line using Lipofectamine (Invitrogen Corp.). After 24 h, cells were challenged with puromycin (2 μg/mL) in complete growth medium and incubated at 37°C for 5 days. Cell cultures were split into dishes for another 2 days of incubation with the drug. Afterwards, medium was replaced with fresh growth medium containing 5% FBS, and cells were incubated at 30°C for 24 h. Culture medium was collected after centrifuging (5 min at 2,000 rpm) and passing through 0.45-Am filters, saved at –80°C as a recombinant virus stock, then used for infection.

Prostate cancer cells were seeded at 500,000 per 100-mm plate in 10 mL of complete medium. Twenty-four hours later, growth medium was removed. Viral stock (2 mL) was added to cells in the presence of 10 μg/mL polybrene (Chemicon International) and incubated for 6 h at 37°C. Then, complete medium (8 mL) was added. Three days postinfection, cells were split (1 to 5-20 dilution) into selection medium containing puromycin (1 μg/mL), and medium was changed every 3 to 4 days until surviving clones were picked and then expanded. Western blotting with Rad9 antibodies was used to assess protein levels for selection of clones demonstrating reduction in Rad9 protein abundance.

Results

Rad9 RNA and encoded protein levels are high in prostate cancer cells

To assess the relationship between *Rad9* and prostate cancer, the level of the encoded protein was examined in four human prostate cancer cell lines, CWR22, DU145, LNCaP, and PC-3, as well as in PrEC normal prostate epithelial cells. Western analyses indicate that Rad9 protein is highly abundant in all the cancer cells, relative to PrEC (Fig. 1*A*). Densitometric analyses of Rad9 to β-actin (internal control) band intensity ratios for each sample performed thrice and averaged indicate an increase in Rad9 protein ranging from 7.8-fold to 15.5-fold in the prostate cancer versus noncancer cells (Fig. 1*B*; specific increases: PC-3, 7.8-fold; LNCaP, 10-fold; DU145, 10-fold; CWR22, 15.5-fold). Immunohistochemical studies confirm these results (Fig. 1*C*).

Rad9 CpG islands are hypermethylated in DU145 cells

Methylation of CpG islands can control gene expression (31, 32). Cheng and coworkers (27) reported that CpG islands within the second intron of *Rad9* might have transcription repressor activity, and methylation of cytosines at those sites neutralize this function, resulting in high expression of *Rad9*. We examined methylation status of the promoter, as well as the first and second exon/intron regions of *Rad9* in normal and cancer prostate cells to assess whether aberrant methylation might be responsible for high levels of *Rad9* expression detected. We used bisulfite sequencing to identify methylation in 10 independent clones derived from each cell population of interest. CpG islands within *Rad9* exons and introns of the prostate normal and cancer cells were methylated, but DU145 cells were relatively hypermethylated (Fig. 2*A*). Excessive methylation was reflected in a number of independent clones bearing CpG island methylation (all 10 studied) and a number of methylated sites per clone. For example, one clone (no. 10) contained 10 methylated CpG islands. Hypermethylation in DU145 was confined to CpG sites within the second *Rad9* intron, where the transcription suppressor is located (27). A similar study of the *Rad9* promoter region did not detect any CpG island methylation (data not shown). Bisulfite sequencing also yields DNA sequence information, and no mutation in the promoter or first two exons/introns of *Rad9* in any of these cells was found.

To determine the functional significance of the CpG island methylation, all four cancer and the control cell populations were treated with the demethylating agent 5′-aza-2′-deoxycytidine (0.25 mmol/L). After treatment, the most dramatic reduction in methylation occurred in DU145 cells (compare Fig. 2*A* and *B*), where baseline starting levels were the highest. For this population, before treatment 10 of 10 clones contained methylated CpG islands, whereas, after treatment, only 5 of 10 contained methylated sites and each clone had a reduced number of such sites.

The effects of 5′-aza-2′-deoxycytidine on Rad9 levels were assessed. This chemical dramatically reduced Rad9 protein abundance in DU145 cells (Fig. 3*A*), suggesting that the high level of the protein in the same cells untreated is due to methylation of CpG islands. Similar treatment of the other cell populations did not reduce Rad9 abundance. Use of 5′-aza-2′-deoxycytidine at concentrations above 0.25 mmol/L (up to 1.0 mmol/L) did not alter Rad9 protein levels any differently than when cells were exposed to the 0.25 mmol/L concentration, and the higher levels of the chemical caused cell death in all populations. Quantitative reverse transcription–PCR (RT-PCR; Fig. 3*B*) showed that *Rad9* RNA abundance was commensurate with the encoded protein levels in untreated (Fig. 1*A*–*C*), mock-treated (Fig. 3*A*), and 5′-aza-2′-deoxycytidine–treated (Fig. 3*A*) cells.

Rad9 gene is amplified in PC-3 cells

We used Southern blotting to determine *Rad9* copy number in the four prostate cancer and PrEC noncancerous cells. DNA from these cells was probed with *Rad9* and the β-actin gene (internal control) to assess relative band intensities, which reflect copy number. Figure 3*D* represents the average results for three independent Southern blots and shows the *Rad9*/β-actin band intensity ratios, as determined by densitometric analyses. PC-3 has about twice the amount of *Rad9* as the other cells, suggesting that gene amplification might, at least in part, be responsible for high levels of the RNA and encoded protein observed. Karyotype analyses of PC-3 cells indicated that there was no selective retention of duplicated chromosome 11, where *Rad9* resides, or selective reduction in chromosome 7, where the β-actin gene is located. Therefore, *Rad9*, and not the entire chromosome 11 within which it is embedded, is increased in copy number in PC-3 cells.

Rad9 protein levels are high in prostate cancer tissues

To extend the findings in prostate cancer cells, we examined immunohistochemically primary biopsy material from normal or cancerous prostates for Rad9 protein. Of 339 prostate cancer samples tested, 153 were positive for HRAD9 (45.1%). Of those containing HRAD9, the most intense stain occurred in stages III and IV adenocarcinomas (and two independent metastases), and all stage I–positive, as well as some stage II–positive, samples showed a less intense but clearly detectable signal. In contrast, 2 of 52 normal prostate tissues had just weak HRAD9 protein signals (3.8%). Table 1 summarizes the results. Figure 4 shows what was considered negative (0), weak (+), strong (++), and very intense (+++) HRAD9 protein staining. These data are consistent with the cell culture results and indicate that high levels of HRAD9 are linked to prostate cancer. The statistical significance for relationships between HRAD9-positive staining and cancer and also stain intensity versus stage were tested (33). Groups, as per Table 1, for consideration were simplified. The ++ and +++ staining numbers were combined, as they clearly differ from the 0 and + groups, and few are +++. The metastasis group was excluded from calculations because these are not primary tumors. A P value of <0.001 was then obtained when comparing percentage positive by cancer stage or staining intensity by cancer stage. P values are also <0.001 if stages III and IV are combined. Interestingly, the latter two stages, unlike stages I and II, involve metastatic disease. Although information on cancer grade was much more limited, there was a good correlation between severity of grade and levels of Rad9 protein (data not shown).

siRNA-mediated decrease in Rad9 protein levels reduces tumorigenicity of human prostate cancer cells

We next tested if there was not just a simple association between high HRAD9 protein levels and prostate cancer, but whether HRAD9 played a functional role in the disease. We used a mouse tumor model system (34). The strategy involved knocking down HRAD9 levels in prostate tumor cells using siRNA and testing whether that would reduce or eliminate tumor formation postinjection into nude mice.

Three human prostate cancer cell lines, CWR22, DU145, and PC-3, as well as noncancerous prostate PrEC cells, were injected at 6×10^6 cells per site subcutis into backs of nude mice (Harlan Sprague-Dawley, Inc.; Nu/Nu male, 4 weeks of age) at eight to nine independent sites per cell population. Matrigel is required for LNCaP cells to form tumors in nude mice, because they are not as aggressive as the other three populations, CWR22, DU-145, and PC-3. Therefore, the LNCaP cell line was not pursued for the tumor-related experiments. Two sites per animal were usually used to reduce the number of mice needed. Pilot tests showed that number of injection sites per animal, from one up to four, did not influence tumor formation frequency or growth. After 2 to 3 weeks, CWR22, DU145, and PC-3 cells formed tumors at each injection site, but PrEC did not. Tumors were of human origin because they stained positive for human epithelial cell markers (cytokeratin 5, 18, 19; Sigma). To test the significance of high Rad9 protein levels with respect to tumorigenicity, CWR22, DU145, and PC-3 cancer cells were stably transfected with insertless pSUPER.retro.puro or one bearing *HRAD9* siRNA. The siRNA was most effective in reducing levels of HRAD9 protein in DU145 cells, followed by reduction in PC-3 (Fig. 5A). siRNA was least effective in CWR22. Densitometric scanning of HRAD9 and β-actin (control) bands indicates that reduction in HRAD9 levels, relative to untransfected or insertless vector controls, was by 86% for DU145 (two independent clones), 76% for PC-3 (one clone), and only by 34% for CWR22 (two different clones).

Vector-bearing or siRNA-bearing cells were injected into nude mice, and animals were examined for tumor development. Tumor size (mm^3) versus days of postinjection is

presented in Fig. 5*B–D*. Mice injected with DU145 cells containing insertless vector (Fig. 5*B*, first four columns in each group) formed detectable tumors starting at day 20, which continued to grow until day 35 (last day of monitoring). However, sites injected with siRNA-containing DU145 cells contained no abnormal growths. These sites were monitored for 5 months, and still no tumors formed. Sites injected with PC-3 cells bearing insertless vector developed tumors that grew progressively during 35 days postinjection (Fig. 5*C*, first five columns in each group). Interestingly, sites containing the same parental cells but with pSUPER.retro.puro *Rad9* siRNA, which reduced levels of the protein significantly but not as dramatically as for DU145, developed small masses by day 20, but they stopped growing shortly thereafter and remained approximately the same size through day 35 (Fig. 5*C*, last seven columns of each group). In contrast, for CWR22 cells with insertless vector and high Rad9 levels, tumors grew so aggressively that, by day 25, the experiment was terminated (Fig. 5*D*, first seven columns in each group). siRNA was not very effective in reducing Rad9 protein levels in CWR22, and for most independent siRNA transfectants, tumors grew aggressively at injection sites (Fig. 5*D*, last six columns). Some variabilities in tumor size and growth rate were observed for all injections of similar cells, and this could reflect differences in mice, differences in exact numbers of cells injected, internal growth of tumors not easily measurable *in vivo*, or changes in Rad9 levels postinjection. However, examination of thin sections of several tumors that formed indicated that levels of Rad9 protein were similar to those observed in the parental cells *in vitro*. Nevertheless, it is clear that, in general, the more Rad9 protein present in prostate cancer cells the more avidly they form tumors when injected into nude mice, indicating a functional relationship between Rad9 abundance and prostate cancer. Furthermore, overexpression of Rad9 in the nontumorigenic, immortalized human prostate cell line PWR-1E conferred upon those cells the ability to form aberrant growths 2 weeks postinjection, although about 2 to 3 weeks later, many began to regress. Specifically, 10 of the 14 sites injected with PWR-1E cells overproducing human Rad9 formed an abnormal growth. In contrast, no abnormal growths formed in six sites injected with parental PWR-1E cells, and only 1 of 12 sites injected with PWR-1E containing an insertless vector control formed a small growth that regressed after 25 days. These data indicate again a functional role for Rad9 in prostate carcinogenesis.

No correlation between Rad9, AR, and PSA protein levels in relation to tumorigenicity of human prostate cancer cells

Because Rad9 was found previously to interact with AR and modulate its ability to transactivate downstream target genes (25, 26), the relevance of Rad9-AR binding to tumorigenesis was examined. In particular, AR regulates the gene encoding PSA, so we examined levels of this protein in the four human prostate cancer cell lines, CWR22, DU145, LNCaP, and PC-3, as a measure of AR transactivity. These four cell populations are capable of forming tumors in nude mice and have very high levels of Rad9 protein, and reduction of Rad9 abundance in DU145, as well as PC-3, reduces or eliminates the ability to form tumors in nude mice. Only CWR22 and LNCaP have AR protein. Western analyses indicated that only LNCaP had high levels of PSA (data not shown), thus demonstrating that the Rad9-AR interaction is not universally essential for prostate cancer cell tumorigenicity because the presence of AR and high levels of PSA did not correlate with ability to form tumors in nude mice. Thus, the role of Rad9 in prostate cancer is likely unrelated to its relationships with AR and PSA.

Discussion

The *Rad9* gene has many functions that could bear on carcinogenesis, including a role in maintaining genomic integrity and regulating cell cycle checkpoints (9). Rad9 protein can bind AR (25, 26). This protein-protein interaction represses the ability of testosterone to

induce a conformational change in the receptor, to activate a receptor transcription regulatory function, and subsequently to express downstream target genes critical for proper prostate function. Based on these and other functions of Rad9, the relationship between this protein and prostate cancer was examined. We show that four prostate cancer cell lines and 153 of 339 prostate adenocarcinomas have aberrantly high levels of Rad9 protein. There was a significant correlation between stage of prostate adenocarcinoma and level of Rad9, where the protein was most often abundant in advanced stages. Noncancerous prostate control PrEC cells and only 2 of 52 normal prostate tissue samples had very low levels of the protein. This is the first demonstration of a link between Rad9 abundance and prostate cancer.

Overexpression of *Rad9* in prostate cancer cells or tissues suggests that it may act as an oncogene, classically, for example, like *E2F-1* when it is expressed at high levels (35). Genetic loci associated with predisposition to prostate cancer, as well as several tumor suppressor genes and oncogenes mediating sporadic prostate cancer, have been identified (36). Using a mouse model, we show that aberrantly high abundance of Rad9 protein can be critical for tumorigenicity of prostate cancer cells because reduction in the level of the protein decreases tumor formation. Functional and molecular relationships between *Rad9* and other genes known to influence prostate carcinogenesis, especially in the context of normal and cancer prostate tissue activity, need to be determined.

Two mechanisms responsible for high levels of Rad9 in prostate cancer cells have been identified. We provide evidence that, in DU145, hypermethylation of cytosines in CpG islands within the 3′ region of *Rad9* intron 2 is important. Cheng and coworkers (27) describe a repressor of transcription located within 200 bp of this intron between bp 406 and 605, which can be inactivated by methylation, and the *Rad9* gene of DU145 is hypermethylated in this region. Treatment with 5′-aza-2′-deoxycytidine reduces the extent of that methylation and concomitantly reduces Rad9 levels. Therefore, these findings suggest that DU145 has abnormally high levels of Rad9 because of aberrant methylation of CpG islands within intron 2 of the gene. DNA sequence analyses of the promoter and first two exons/introns of *Rad9* in DU145 (also in CWR22, LNCaP, and PC-3) did not reveal a mutation. Therefore, these results suggest that DU145 cells show high levels of Rad9 due to abnormal activity of an upstream regulator of *Rad9*, perhaps a methylase, a demethylase, or a protein that controls these enzymes. Consistent with these findings, preliminary studies indicate that high levels of Rad9 protein are also frequently associated with hypermethylation of the potential transcription suppressor in primary human prostate tumors (data not shown).

The *Rad9* gene was modestly amplified in prostate cancer PC-3 cells, which could account at least in part for high levels of the encoded protein detected. Other investigators reported that *Rad9* copy number was increased in certain breast tumors and contributed to increased expression (27). Therefore, gene amplification in addition to aberrant methylation is a mechanism that can regulate Rad9 protein abundance.

The relevance of the physical interaction of Rad9 and AR, with respect to influence of the former on transactivity of the latter, in the context of prostate cancer is not clear or at least not a universal, biologically significant feature of the disease. For example, LNCaP and CWR22 prostate cancer cells have AR and high levels of Rad9 protein. However, only the former cells have high levels of PSA (data not shown), which is regulated by AR. Furthermore, there is no relationship of the role of Rad9 in prostate cancer to dependence on androgen for growth or tumorigenesis because CWR22 and LNCaP are androgen dependent whereas DU145 and PC-3 are androgen independent, yet they all contain high levels of Rad9 protein and can form tumors in nude mice.

In this report, we show that high levels of Rad9 are associated with prostate cancer and can be critical for tumorigenicity. Other investigators found that *Rad9* overexpression is associated with breast cancer and non–small cell lung carcinoma (27, 37). Despite these results, Rad9 is likely not a universal oncogene linked to cancer of all tissues because preliminary studies indicate no correlation between abundance of Rad9 and cancer of the stomach or colon.[3] However, *Rad9* mutation as a mechanism for contributing to these or other types of cancer has not been ruled out.

At a minimum, our findings support the use of Rad9 as a biomarker for advanced prostate cancer. Further investigations of this kind with Rad9 could lead to the development of better diagnostic, prognostic, and even therapeutic tools to lower the death rate caused by the disease, which is a very significant concern because the incidence is high.

Acknowledgments

Grant support: NIH grants GM079107 and CA130536 (H.B. Lieberman).

The costs of publication of this article were defrayed in part by the payment of page charges. This article must therefore be hereby marked *advertisement* in accordance with 18 U.S.C. Section 1734 solely to indicate this fact.

We thank Drs. Ralph Buttyan and Arther Ko for providing cell lines, Dr. Harshwardhan M. Thaker for aiding in the interpretation of tissue microarray data, Dr. Genze Shao and Xiangyuan Wang for technical advice, Dr. Adayabalam Balajee for performing karyotype analysis, and Drs. William T. Friedewald and Shing Lee for guidance with statistical analyses.

References

1. Suzuki H, Freije D, Nusskern DR, et al. Interfocal heterogeneity of PTEN/MMAC1 gene alterations in multiple metastatic prostate cancer tissues. Cancer Res. 1998; 58:204–9. [PubMed: 9443392]
2. Ellwood-Yen K, Graeber TG, Wongvipat J, et al. Myc-driven murine prostate cancer shares molecular features with human prostate tumors. Cancer Cells. 2003; 4:223–38.
3. DiGiovanni J, Kiguchi K, Frijhoff A, et al. Deregulated expression of insulin-like growth factor 1 in prostate epithelium leads to neoplasia in transgenic mice. Proc Natl Acad Sci U S A. 2000; 97:3455–60. [PubMed: 10737798]
4. Terry S, Yang X, Chen MW, Vacherot F, Buttyan R. Multifaceted interaction between the androgen and Wnt signaling pathways and the implication for prostate cancer. J Cell Biochem. 2006; 99:402–10. [PubMed: 16741972]
5. Kasper S. Survey of genetically engineered mouse models for prostate cancer: analyzing the molecular basis of prostate cancer development, progression, and metastasis. J Cell Biochem. 2005; 94:279–97. [PubMed: 15565647]
6. Klein RD. The use of genetically engineered mouse models of prostate cancer for nutrition and cancer chemoprevention research. Mutat Res. 2005; 576:111–9. [PubMed: 15885713]
7. Paris PL, Andaya A, Fridly J, et al. Whole genome scanning identifies genotypes associated with recurrence and metastasis in prostate tumors. Hum Mol Genet. 2004; 13:1303–13. [PubMed: 15138198]
8. Lieberman HB, Hopkins KM, Nass M, Demetrick D, Davey S. A human homolog of the *Schizosaccharomyces pombe rad9+* checkpoint control gene. Proc Natl Acad Sci U S A. 1996; 93:13890–5. [PubMed: 8943031]
9. Lieberman HB. *Rad9*, an evolutionarily conserved gene with multiple functions for preserving genomic integrity. J Cell Biochem. 2006; 97:690–7. [PubMed: 16365875]
10. Komatsu K, Miyashita T, Hang H, et al. Human homologue of S. pombe Rad9 interacts with Bcl-2/Bcl-XL and promotes apoptosis. Nat Cell Biol. 2000; 2:1–6. [PubMed: 10620799]

[3]A. Zhu and H.B. Lieberman, unpublished data.

11. Hopkins KM, Auerbach W, Wang XY, et al. Deletion of mouse Rad9 causes abnormal cellular responses to DNA damage, genomic instability, and embryonic lethality. Mol Cell Biol. 2004; 16:7235–48. [PubMed: 15282322]
12. Bessho T, Sancar A. Human DNA damage checkpoint protein hRAD9 is a 3′ to 5′ exonuclease. J Biol Chem. 2000; 275:7451–4. [PubMed: 10713044]
13. Yin Y, Zhu A, Jin YJ, et al. Human RAD9 checkpoint control/proapoptotic protein can activate transcription of *p21*. Proc Natl Acad Sci U S A. 2004; 101:8864–9. [PubMed: 15184659]
14. Lieberman HB, Yin Y. A novel function for human Rad9 protein as a transcriptional activator of gene expression. Cell Cycle. 2004; 3:1008–10. [PubMed: 15280665]
15. Ishikawa K, Ishii H, Murakumo Y, et al. Rad9 modulates the P21WAF1 pathway by direct association with p53. BMC Mol Biol. 2007; 18:37–46. [PubMed: 17511890]
16. Lindsey-Boltz LA, Wauson EM, Graves LM, Sancar A. The human Rad9 checkpoint protein stimulates the carbamoyl phosphate synthetase activity of the multi-functional protein CAD. Nucleic Acids Res. 2004; 32:4524–30. [PubMed: 15326225]
17. Toueille M, El-Andaloussi N, Frouin I, et al. The human Rad9/Rad1/Hus1 damage sensor clamp interacts with DNA polymerase β and increases its DNA substrate utilisation efficiency: implications for DNA repair. Nucleic Acids Res. 2004; 32:3316–24. [PubMed: 15314187]
18. Wang W, Brandt P, Rossi ML, et al. The human Rad9-1-Hus1 checkpoint complex stimulates flap endonuclease 1. Proc Natl Acad Sci U S A. 2004; 101:16762–7. [PubMed: 15556996]
19. Friedrich-Heineken E, Toueille M, Tännler B, et al. The two DNA clamps Rad9/Rad1/Hus1 complex and proliferating cell nuclear antigen differentially regulate Flap endonuclease 1 activity. J Mol Biol. 2005; 353:980–9. [PubMed: 16216273]
20. Helt CE, Wang W, Keng PC, Bambara RA. Evidence that DNA damage detection machinery participates in DNA repair. Cell Cycle. 2005; 4:529–32. [PubMed: 15876866]
21. Smirnova E, Toueille M, Markkanen E, Hübsche U. The human checkpoint sensor and alternative DNA clamp Rad9/Rad1/Hus1 modulates the activity of DNA ligase I, a component of the long patch base excision repair machinery. Biochem J. 2005; 389:13–7. [PubMed: 15871698]
22. Wang W, Lindsey-Boltz LA, Sancar A, Bambara RA. Mechanism of stimulation of human DNA ligase I by the rad9-1-hus1 checkpoint complex. J Biol Chem. 2006; 281:20865–72. [PubMed: 16731526]
23. Gembka A, Toueille M, Smirnova E, et al. The checkpoint clamp, Rad9-1-Hus1 complex, preferentially stimulates the activity of apurinic/apyrimidinic endonuclease 1 and DNA polymerase {β] in long patch base excision repair. Nucleic Acids Res. 2007; 35:2596–608. [PubMed: 17426133]
24. Pandita RK, Sharma G, Laszlo A, et al. Mammalian Rad9 plays a role in telomere stability, S- and G_2-phase specific cell survival and homologous recombinational repair. Mol Cell Biol. 2006; 26:1850–64. [PubMed: 16479004]
25. Wang L, Hsu CL, Ni J, et al. Human checkpoint protein hRad9 functions as a negative coregulator to repress androgen receptor transactivation in prostate cancer cells. Mol Cell Biol. 2004; 24:2202–13. [PubMed: 14966297]
26. Hsu C- L, Chen Y- L, Ting H- J, et al. Androgen receptor (AR) NH2- and COOH-terminal interactions result in the differential influences on the AR-mediated transactivation and cell growth. Mol Endocrinol. 2005; 19:350–61. [PubMed: 15514032]
27. Cheng CK, Chow LW, Loo WT, Chan TK, Chan V. The cell cycle checkpoint gene *Rad9* is a novel oncogene activated by 11q13 amplification and DNA methylation in breast cancer. Cancer Res. 2005; 65:8646–54. [PubMed: 16204032]
28. Zhao YL, Piao CQ, Wu LJ, et al. Differentially expressed genes in asbestos-induced tumorigenic human bronchial epithelial cells: implication for mechanism. Carcinogenesis. 2000; 21:2005–10. [PubMed: 11062161]
29. Shao G, Berenguer J, Borczuk AC, Powell CA, Hei TK, Zhao Y. Epigenetic inactivation of βig-h3 gene in human cancer cells. Cancer Res. 2006; 66:4566–73. [PubMed: 16651406]
30. Takai D, Jones PA. Comprehensive analysis of CpG island in human chromosomes 21 and 22. Proc Natl Acad Sci U S A. 2002; 99:3740–5. [PubMed: 11891299]

31. Strathdee G, Sim A, Brown R. Control of gene expression by CpG island methylation in normal cells. Biochem Soc Trans. 2004; 32:913–5. [PubMed: 15506922]

32. Klose RJ, Bird AP. Genomic DNA methylation: the mark and its mediators. Trends Biochem Sci. 2006; 31:89–97. [PubMed: 16403636]

33. Zar, JH. Biostatistical Analysis. 4th ed.. Upper Saddle River; Prentice Hall: 1999. p. 555-7.

34. Bex A, Lummen G, Rembrink K, Otto T, Metz K, Rubben H. Influence of pertussis toxine on local progression and metastasis after orthotopic implantation of the human prostate cancer cell line PC3 in nude mice. Prostate Cancer Prostatic Dis. 1999; 2:36–40. [PubMed: 12496864]

35. Johnson DG, Cress WD, Jakio L, Nevins JR. Oncogenic capacity of the E2F1 gene. Proc Natl Acad Sci U S A. 1994; 91:12823–7. [PubMed: 7809128]

36. Shand RL, Gelmann EP. Molecular biology of prostate-cancer pathogenesis. Curr Opin Urol. 2006; 16:123–31. [PubMed: 16679847]

37. Maniwa Y, Yoshimura M, Bermudez VP, et al. Accumulation of hRad9 protein in the nuclei of nonsmall cell lung carcinoma cells. Cancer. 2005; 103:126–32. [PubMed: 15558813]

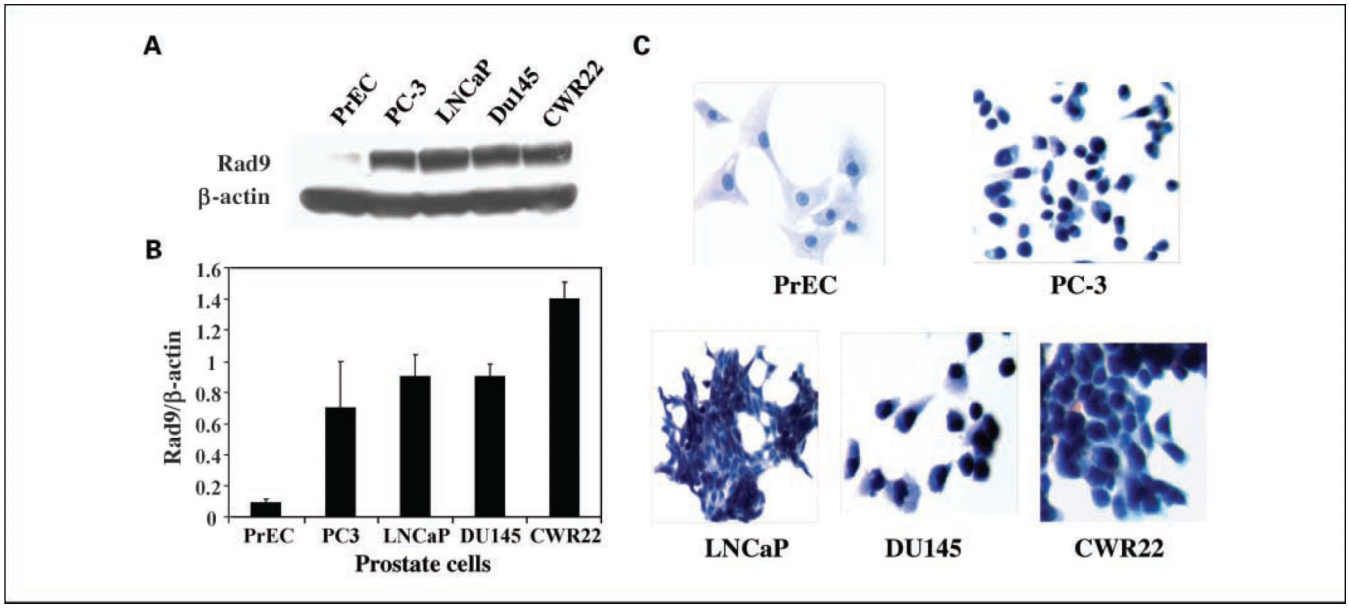

Figure 1.

Rad9 expression in normal and prostate cancer cell lines. *A*, Western analyses for Rad9 and β-actin proteins in extracts from normal (PrEC) and cancerous (PC-3, LNCaP, DU145, and CWR22) prostate cells. *B*, graph of Rad9/β-actin band intensity ratios for the samples in *A*. *C*, immunohistochemical staining for Rad9 protein in normal and prostate cancer cells. Note the heavily stained nuclei indicative of Rad9 in the cancer cell lines, relative to the more lightly stained PrEC noncancerous control cell population.

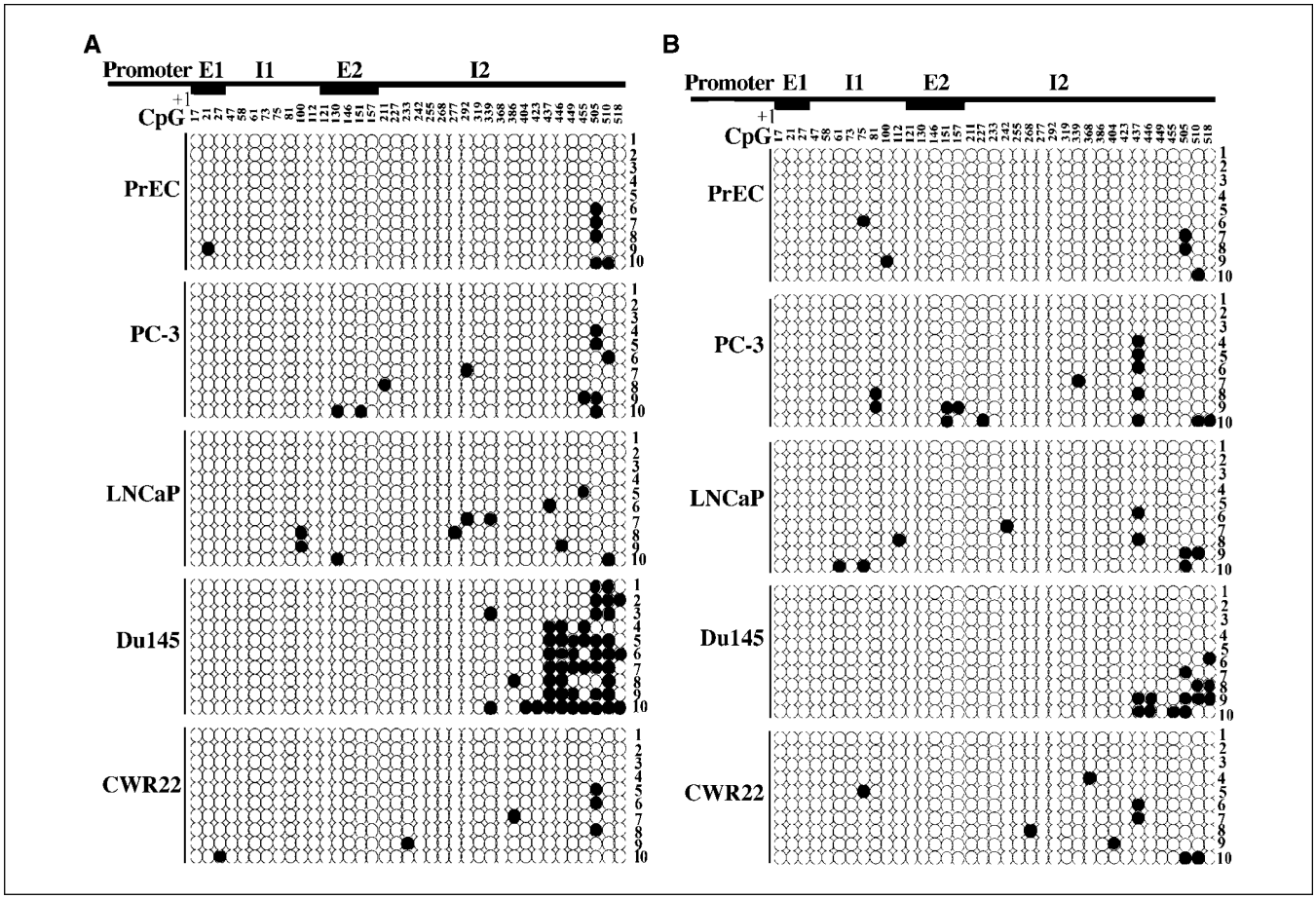

Figure 2.

Methylation patterns of *Rad9* CpG islands in normal and prostate cancer cells. *A*, cells growing in log phase. *B*, same as in *A* but cells were treated with 5′-aza-2′-deoxycytidine (0.25 mmol/L). *Black dots*, cytosine methylation within the designated CpG island. *E1*, exon 1; *I1*, intron 1; *E2*, exon 2; *I2*, intron 2. The start of translation, denoted as +1, is the beginning of the first ATG in exon 1.

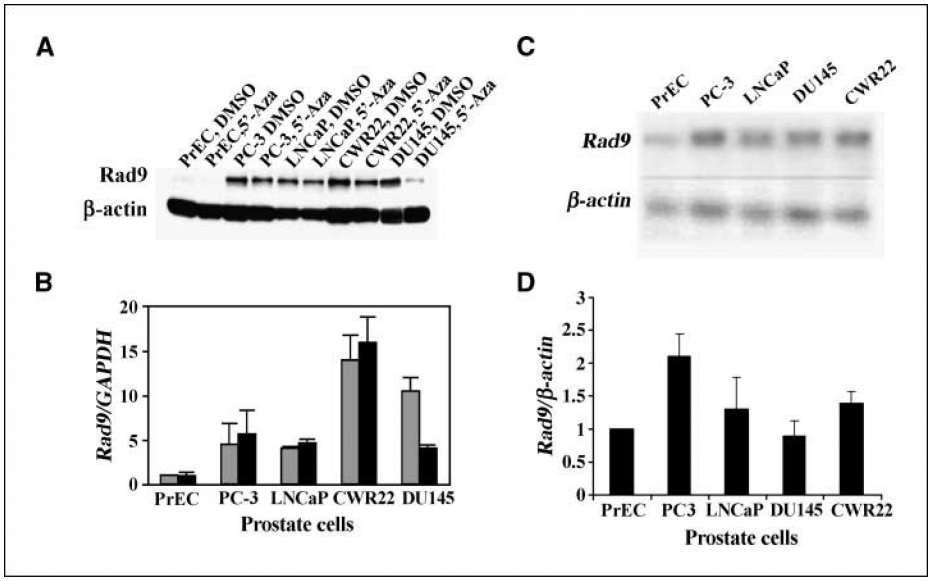

Figure 3.

Mechanism of *Rad9* overexpression. *A*, effect of 5′-aza-2′-deoxycytidine treatment on Rad9 protein levels in PrEC, PC-3, LNCaP, CWR22, and DU145 cells. *B*, quantitative RT-PCR for *Rad9* RNA levels in cells mock-treated or treated with 5′-aza-2′-deoxycytidine. *Gray columns*, mock treatment; *black columns*, 5′-aza-2′-deoxycytidine treatment. Ratios of *Rad9* to the *GAPDH* internal control RNA in each sample are indicated. *C*, Southern blot indicating intensities of *Rad9* and *β-actin* DNA bands in cells. *D*, ratios of *Rad9* to *β-actin* bands DNA quantified and presented relative to the ratio in PrEC.

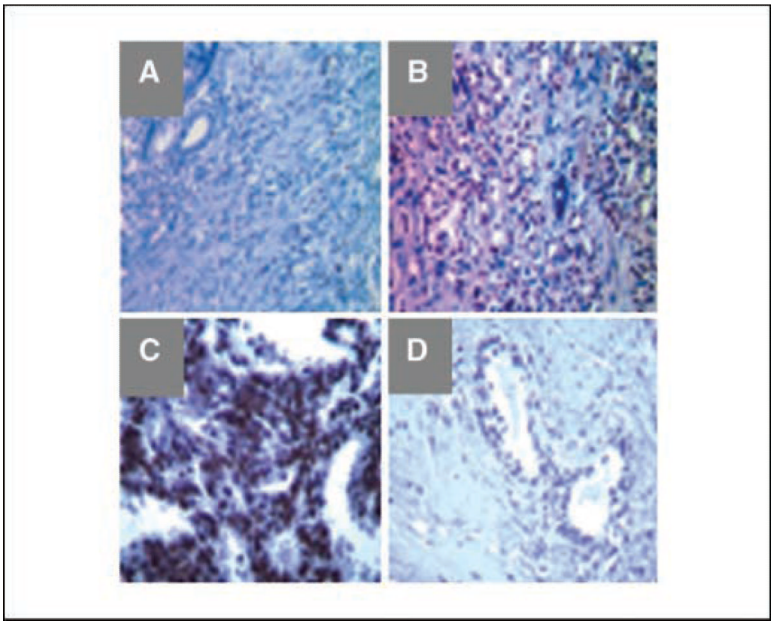

Figure 4.

Immunohistochemical staining for HRAD9 protein in thin sections of prostate tissue. *A*, adenocarcinoma, stage III, weak staining (+) for HRAD9 protein. *B*, adenocarcinoma, stage III, strong staining (++) for HRAD9. *C*, adenocarcinoma, stage IV, very intense stain (+++). *D*, normal, noncancerous prostate tissue, no detectable HRAD9 stain. *Brown stain*, HRAD9 protein; *blue areas*, negative.

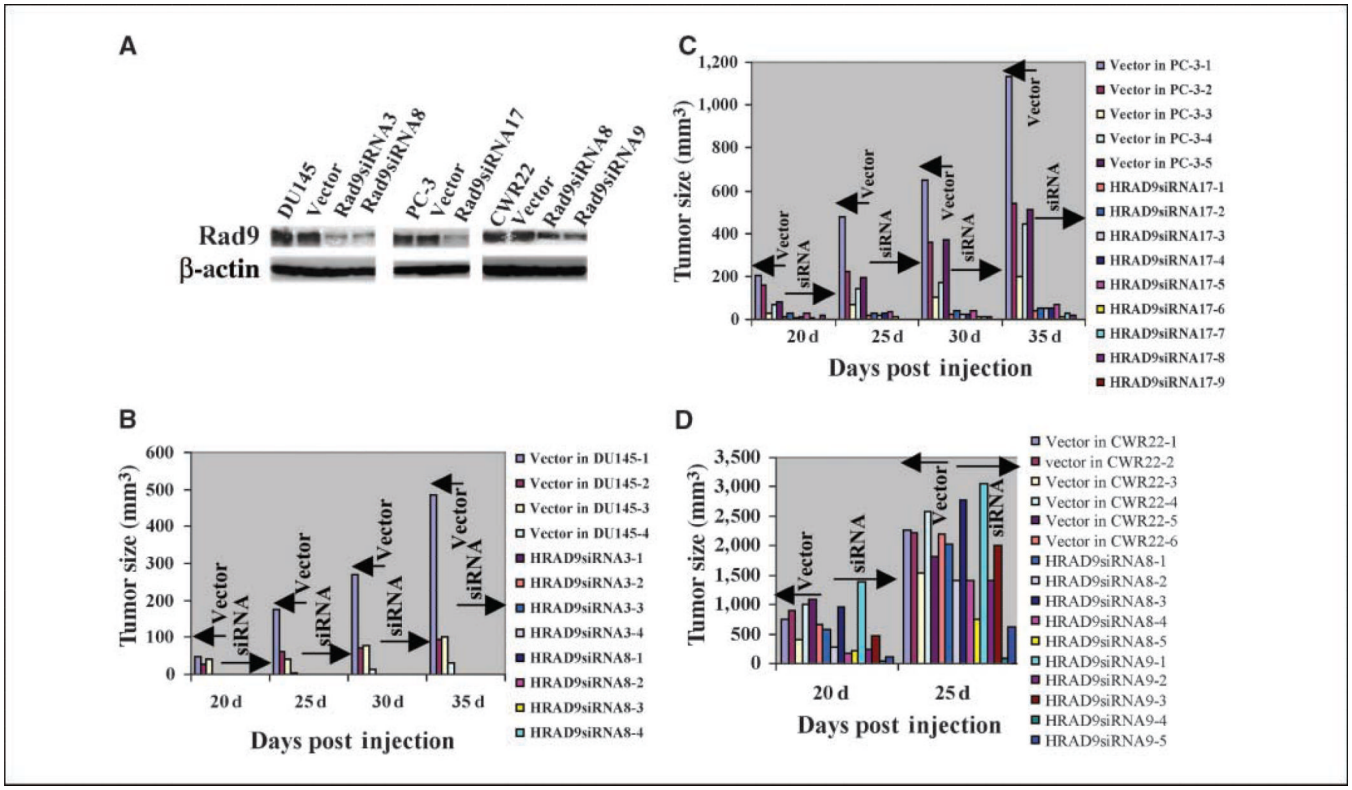

Figure 5.

Reduction of HRAD9 levels in prostate cancer cells reduces tumorigenicity. *A*, Western blots indicating reduction of HRAD9 protein in prostate cancer cells. *Left*, DU145 cells untransfected, with insertless vector, and two stable clones with *HRAD9* siRNA; *middle*, PC3 cells, same as in the left but showing only one independent clone; *right*, CWR22 cells, similar to left. *HRAD9* siRNA was most effective in reducing levels of the protein in DU145 and PC3 cells and least effective in CWR22 cells. The cells as per *A* were injected into multiple sites in the backs of nude mice subcutis. Tumor formation was monitored up to 35 d, except for CWR22, wherein tumors grew so aggressively, the experiment was terminated on day 25. *B*, injection of DU145 cells with insertless vector or *HRAD9* siRNA. *C*, injection of PC3 cells as per *B*. *D*, injection of CWR22 cells as per *B*. There was a direct dose-dependent relationship between HRAD9 levels and tumor growth; the less Rad9, the fewer tumors. Each column is a single site injection. Sites injected with DU145 cells + *Rad9* siRNA were monitored for 5 mo beyond the data shown, and still no tumors formed. *Arrows above columns*, empty vector control or siRNA transformants.

Table 1

Immunohistochemical staining for Rad9 protein in normal and cancer prostate tissue

Cancer stage	No. cases	Stain*				Positive staining (%)
		0	+	++	+++	
Normal	52	50	2			3.8%
I	43	33	10			23.3%
II	65	38	23	4		41.5%
III	155	79	52	24		49%
IV	72	36	25	8	3	50%
Metastasis	4	0	2	0	2	100%
Prostate cancer cases	339					
Positive cases	153					45.1%

*Degree of human HRAD9 protein positive staining: 0, undetectable; +, weak positive; ++, strong positive; +++, very intense staining. See Fig. 4 for examples.